Calculation of the average melting rate of precipitation particles.

I.V.Akimov
Hydrometeorological Centre of Russia
11-13 Bolshoy Predtechensky per., 123242, Moscow-242, Russia.
E-mail: akimov@rhmc.mecom.ru

The definition of the average melting rate of precipitation particles is the important problem originating at prediction of such meteorological phenomenon as wet snow, hail, ice-crusted ground etc. The average melting rate E_M depends on temperature profile near the surface, precipitation particles size and their fall velocity. The most common way to define E_M is receiving it as mean from particles mass variance following formula:

$$E_M = \int_0^\infty \left(\frac{dm}{dt}\right)_M N(r)dr\,, \qquad (1)$$

where $N(r)$ is the distribution function of precipitation particles. The expression of mass variance of precipitation particle due to melting process has the next form [1]:

$$\left(\frac{dm}{dt}\right)_M = \frac{4\pi r k}{L_f} C(T - T_s)\,, \qquad (2)$$

where r - equivalent radius of precipitation particle, L_f - latent heat of melting, k -heat conductivity coefficient of air, T - temperature in the atmosphere, T_s - temperature on the surface of the particle, $C = 1.6 + 0.3 \cdot \mathrm{Re}^{1/2}$, where Re is Reynolds number.

Fall velocity of precipitation particles is calculated by the following formula:

$$U(r) = k_2 \sqrt{r}\ , \qquad (3)$$

where $k_2 = 2 \cdot 10^2$ $\mathrm{m}^{1/2}$ /s .

Using the formula (2) for $(dm/dt)_M$ and assumed $N(r)$ as a gamma function with two parameters [2], after solving the integral in (1) we can receive the following formula for E_M:

$$E_M = \frac{3\delta_{PRES}}{\rho_W r_0^2} \frac{k}{L_f} (T - T_s) \left(\frac{c}{(\mu+2)(\mu+3)} + d \cdot r_0^{3/4} \frac{\Gamma(\mu + 2.75)}{\Gamma(\mu+4)} \right) \qquad (4)$$

where δ_{PRES} is summary water content (liquid water and ice) of precipitation, r_0 is the mean equivalent radius of precipitation particles, μ is the gamma distribution parameter, assumed as $\mu = 0.41$ accordingly to the work [2], ρ_W is the density of water, $c = 1.6$, $d = 0.3 \cdot (2\rho k_2 / \eta)^{1/2} = 1920.0$ $\mathrm{m}^{-3/4}$ are the constants.

The results of average melting rate calculation in dependence of different values of temperature in the atmosphere are presented in the left part of Table 1. The calculations were conducted with constant value of summary water content of precipitation $\delta_{PRES} = 0.3$ $\mathrm{g/m}^3$, and different values of mean equivalent radius of precipitation particles - r_0. Results presented in the right part of the table are the values of time $t_M = \delta_{PRES} / E_M$ during which the precipitation particles are completely melted (as a numerator of fraction) and the values of path in the atmosphere $z_M = \overline{U}(r_0) \cdot t_M$ during which melting of precipitation particles occurs (as a denominator of fraction). The values of mean fall velocity of precipitation particles $\overline{U}(r_0)$ and

time interval $\Delta\tau$ which needed for precipitation particles to reach the surface from 925 gPa level are presented at the bottom of the table.

The table allow to analyse at what temperatures and mean radius values precipitation can reach the surface as wet snow. The result of comparison of fall time $\Delta\tau$ with melting time t_M under different values of mean radius r_0 shows that precipitation with mean radius $r_0 = 350$ mkm can reach the surface as a wet snow only at temperatures in $1000 \div 925$ gPa level is lower than $1.5°C$. Precipitation with greater mean radius $r_0 = 350$ mkm can reach the surface as a wet snow then the temperatures near the surface is lower than $3°C$. When precipitation has smaller mean radius $r_0 = 200$ mkm particles reach the surface as completely melted at all temperatures near the surface.

The results presented in Table 1 shows that wet snow occurs only at small positive temperatures near the surface and occurrence of this phenomenon depends strongly from values of mean radius of precipitation particles.

Table 1.

Dependence of average melting rate from temperatures near the surface and mean radius values for precipitation which fall out from 925 gPa level.

$t°C$	E_T g/m^{3}c $\cdot 10^2$			t_T min/ z_T km		
	$r_0 = 200$	$r_0 = 350$	$r_0 = 500$	$r_0 = 200$	$r_0 = 350$	$r_0 = 500$
1	0.26	0.12	0.074	2.12 0.32	4.11 0.90	6.75 1.82
2	0.52	0.24	0.15	1.06 0.16	2.06 0.45	3.38 0.91
3	0.78	0.36	0.22	0.67 0.11	1.46 0.30	2.31 0.61
4	1.04	0.48	0.30	0.53 0.08	1.03 0.22	1.69 0.45
5	1.30	0.60	0.37	0.40 0.06	0.86 0.18	1.45 0.36
$\Delta\tau$ min				3.6	2.6	2.3
$\bar{V}$ m/s				2.8	3.6	4.5

References:

1. Mason B. J., 1957: The physics of clouds. Oxford. At the Clarendon press, 542 p.

2. Shlesinger M.E., Oh J.H., Rosenfeld O., 1986: A parameterization of the evaporation of rainfall. Monthly Weather Review, v.116, N 10, pp. 1887-1895.

OPERATIONAL IMPLEMENTATION of the ISBA LAND SURFACE SCHEME in the CANADIAN REGIONAL FORECAST MODEL

Stéphane Bélair[*], Jocelyn Mailhot[*], Yves Delage[*], Ross Brown[*], Louis−Philippe Crevier[**], and Bernard Bilodeau[*]

[*]*Meteorological Research Branch, Meteorological Service of Canada*
[**]*Canadian Meteorological Centre, Meteorological Service of Canada*

In September 2001, a new surface modeling and assimilation strategy was operationally implemented into the Canadian regional weather forecasting system. The surface processes over land are evaluated in this system using the ISBA landsurface scheme (Noilhan and Planton 1989). Surface variables, including soil moisture, are initialized using a sequential assimilation technique in which model errors on low−level air temperature and relative humidity are used to determine innovations on surface variables.

It was found, for summertime results (see Bélair et al. 2002a), that the magnitude and nature of the corrections applied to the surface variables depend on the surface and meteorological conditions observed in each region. For regions with less meteorological activity, model errors on low−level air characteristics were more likely to be related to incorrect representation of surface processes due to either erroneous initial conditions or inaccurate parameterizations in the landsurface scheme. For other regions with more frequent and more intense precipitation events, surface corrections were mainly associated with inacurrate atmospheric forcing.

Objective evaluation against observations from radiosondes and surface stations showed that the amplitude of the diurnal cycle of near−surface air temperature and humidity is larger with the new surface system, in better agreement with observations. This type of improvement was found to extend higher−up in the boundary layer (up to 700 hPa) where cold and humid biases were significantly reduced by introducing the new surface system (e.g., see Fig. 1). The model precipitation was also found to be significantly improved by the new representation of surface fluxes (i.e., decrease of a positive bias)

The performance of a modified version ISBA's snow scheme, was also examined (see Bélair et al. 2002b). The stand−alone verification tests that were conducted prior to the operational implementation show that ISBA's new snow package was able to realistically reproduce the main characteristics of snow, such as snow water equivalent and density, for 5 winter datasets taken at Col−de−Porte, France, and at Goose Bay, Canada (e.g., see Fig. 2). The results further revealed the manner in which each of the modification that was included into ISBA's snow model (i.e., new liquid water reservoir in the snow pack, new formulation of snow density, and melting effect of incident rainfall on the snow pack) contributed in improving the numerical representation of snow's characteristics. This type of improvement was not found for liquid water runoff under the snow pack and for snow's superficial temperature.

Objective scores for the fully−interactive pre−implementation tests that were done with the Canadian regional weather forecast model indicated that using ISBA's new snow scheme instead of the highly−parameterized snow model that was previously used operationally at CMC only had minor impacts on the model's ability to predict atmospheric circulations. The objective scores revealed that only a thin atmospheric layer above snow−covered surfaces was influenced by the change of landsurface scheme, and that over these regions the essential behavior of the atmospheric model was not significantly altered by the change of landsurface scheme.

Bélair, S., L−P. Crevier, J. Mailhot, B. Bilodeau, and Y. Delage, 2002a: Operational implementation of the ISBA surface scheme in the Canadian regional weather forecast model: Warm season results. To be submitted to *J. Hydromet.*

Bélair, S., R. Brown, J. Mailhot, L.−P. Crevier, and B. Bilodeau, 2002b: Operational implementation of the ISBA surface scheme in the Canadian regional weather forecast model: Cold season results. To be submitted to *J. Hydromet.*

Noilhan, J., and S. Planton, 1989: A simple parameterization of land surface processes for meteorological models. *Mon. Wea. Rev.*, **117**, 536−549.

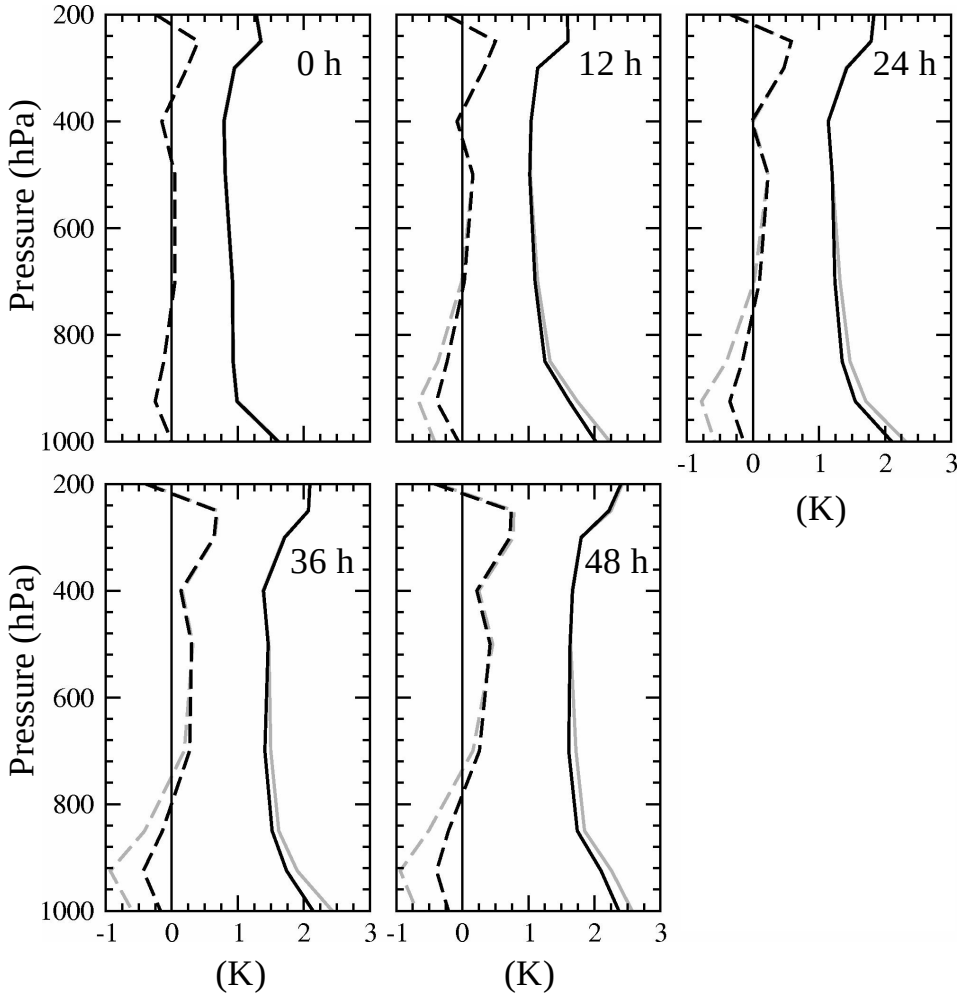

Fig. 1. Objective evaluation of upper−air temperature for 18 cases of August 2000. Root−mean−square (K, full lines) and bias (K, dashed lines) errors are shown for 0−h, 12−h, 24−h, 36−h, and 48−h forecasts from the operational (grey lines) and parallel (black lines) cycles.

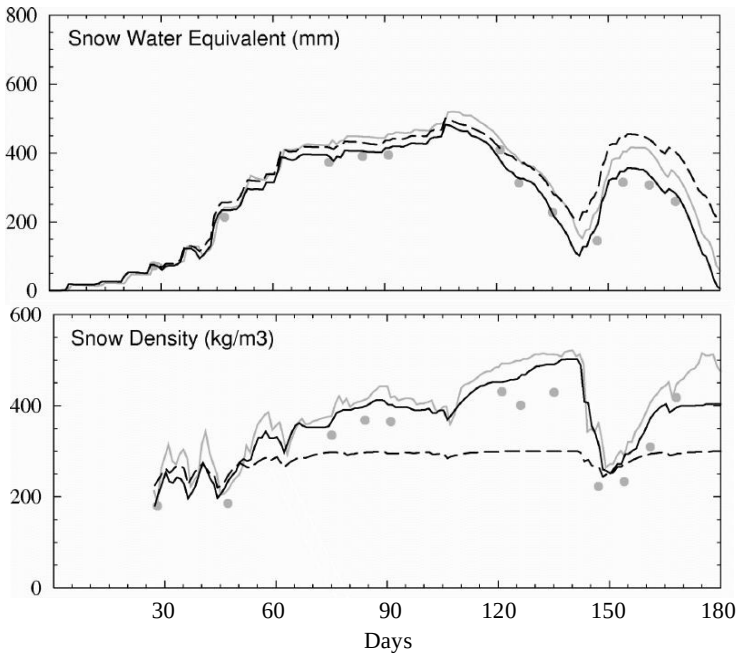

Fig. 2. Comparison between simulated and observed snow characteristics for winter 1993/94 at Col−de−Porte, France. Results from new and original ISBA snow models (full and dashed black lines, respectively) and CROCUS (full grey lines) are shown. The large grey dots represent observations.

Developments on the snow parameterization in ARPEGE

E. Bazile[1], M. ElHaiti, A. Bogatchev and V. Spiridonov
Météo-France/CNRM

In the NWP ARPEGE model, the snow cover fraction (P_{sn}) is a simple function of the snow quantity, represented by its equivalent water content (W_n): $P_{sn} = W_n/(W_n + 10)$. The snow fraction is crucial for the computation of the total surface albedo, owing to the fact that it is a combination of the initial surface albedo (~ 0.15) and the snow albedo ($\alpha_{sn} \sim 0.7$). [VB99] have decreased the cold bias on the boreal forest present in the ECMWF model with the use of the forest albedo instead of the snow albedo. The current modification goes further, with a snow cover fraction on vegetation part function of the leaf area index but also of the snow age. A prognostic equation for the snow albedo will be added to parametrize the ageing process on the albedo as proposed by [DRM95].

In ARPEGE, the general bias over the snow cover areas is positive, but on the forests in the Northern America a cold bias appears. It is clearly linked with the boreal forest with a Leaf Area Index (LAI) greater than 3.5. Therefore the idea of considering the albedo of the vegetation to reduce the cold bias on the forests seems to be justified. In addition, a prognostic equation for the snow albedo will afford the possibility to increase the albedo up to 0.85 with fresh snow instead of 0.7 (as presently fixed in operations), and consequently reduce the warm bias. To take into account the snow below the canopy in forests, fallen from the leaves, a relative snow cover fraction on the vegetation was introduced (P_{sn}^{veg}). P_{sn}^{veg} should be smaller than the equivalent over bareground (P_{sn}^{bg}) and we assume $P_{sn}^{veg} = P_{sn}^{bg} * F$. F is a decreasing function of both the Leaf Area Index and the snow age. For low vegetation ($LAI < 3$) F is equal to 1 and for forest ($LAI \geq 3$) the function F may decrease down to 0.15.

- $F(Lai, \alpha_{sn}) = 1$ for $LAI < 3$
- $F(Lai, \alpha_{sn}) = 1 - \frac{LAI}{K_{lai}} \cdot \frac{\alpha_1 - max(\alpha_0, \alpha_{sn})}{\alpha_1 - \alpha_0}$ for $LAI > 3$, $\alpha_1 = 0.87$, $\alpha_0 = 0.84$, $K_{lai} = 7$

The parameter α_0 was tuned to 0.84 so as to obtain a maximum impact between 6 hours and 30 hours after the latest snow fall (more details in [BEBS02]). After a snow fall, the function F could be closed to 1 also for a LAI greater than 3 (fresh snow can remain on the leaves), but [BB97] have shown that the maximum for the forest albedo is rarely larger than 0.3 for conifer and 0.35 for aspen.

A modification on a snow scheme with a new prognostic variable must be tested along a complete winter season, in order to achieve validation during the accumulation and the melting periods of the snow. The validation was made with the 3DVAR for the winter 2000/2001. Scores against SYNOP and TEMP observations were computed. The SYNOP scores on North 20° and EUROPE are roughly equivalent or slightly better than the current scheme. Over Northern America, the improvement is more significant for March and becomes negligible for April (Fig: 1). Scores against TEMP are slightly improved: around 1mgp at 72h for the geopotential over Europe (Fig: 2).

The new scheme improves the 2m temperature over boreal forests in spring and the introduction of the prognostic snow albedo reduces the warm bias over Antarctica. The impact in upper air is also positive but only after one month assimilation cycle !

[1]Météo-France, CNRM/GMAP 42 Av. Coriolis, 31057 Toulouse Cédex, France, eric.bazile@meteo.fr

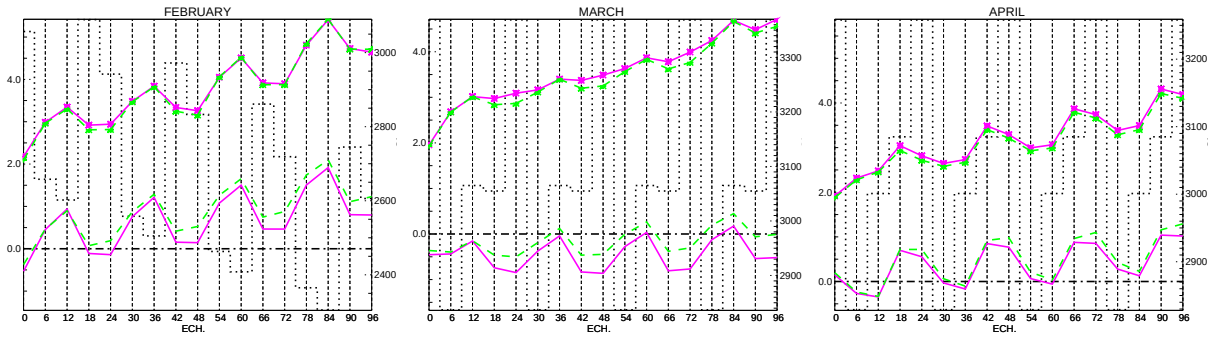

Figure 1: Bias and Rms against SYNOP for T_{2m} over Northern America. Full line: Ref. Dashed line: New.

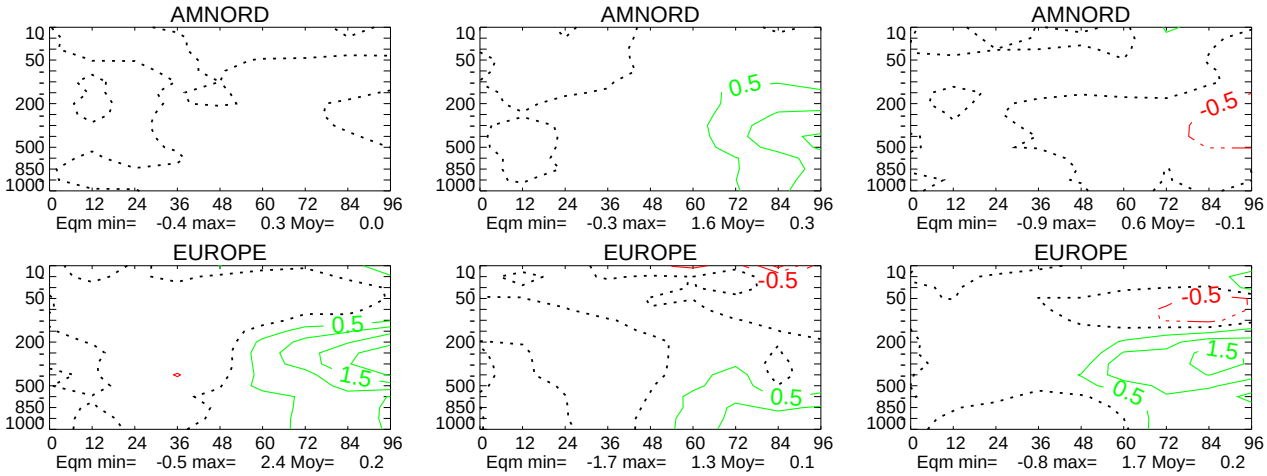

Figure 2: Scores against TEMP. Difference of rms between the reference and the new scheme. X-axis: forecast length. Y-axis: Pressure. Full line: improvement. Dotted line: neutral; Dashed line: deterioration. Left: January. Middle: February. Right: March.

References

[BB97] A.K. Betts and J.H. Ball, *Albedo over the boreal forest*, J. of Geo. Research **102** (1997), 28,901–28,909.

[BEBS02] E. Bazile, M. ElHaiti, A. Bogatchev, and V. Spiridonov, *Improvement of the snow parameterization in ARPEGE/ALADIN*, Proceedings of SRNWP/HIRLAM Workshop, 22-24 October 2001, Madrid, HIRLAM 5 Project, c/o Per Undén, SMHI, S-601 76 Norrköping, SWEDEN, January 2002, pp. 14–19.

[DRM95] H. Douville, J.F. Royer, and J-F. Mahfouf, *A new snow parameterization for the Météo-France climate model, Part 1: Validation in stand-alone experiments, Part II: Validation in a 3D GCM experiment*, Climate Dyn. **12** (1995), 21–52.

[VB99] P. Viterbo and A.K. Betts, *Impact on ECMWF forecasts of changes to the albedo of the boreal forests in the presence of snow*, J. of Geo. Research **104** (1999), 27,803–27,810.

ON THE CLOUD AMOUNT PARAMETERIZATION.

Dmitrieva-Arrago L.R., Anisimova E.V.

Hydrometeorological Scientific Research Centre of Russia,
Bolshoy Predtechensky Per., 11-13, 123242, Moscow, Russia
dmitrieva@rhmc.mecom.ru

Today state of the cloud amount parameterization in the hydrodynamical models of the atmosphere is based upon the relative humidity threshold values that regulate the cloud formation starting, so called relative humidity critical value, f_{cr}. Smagorinsky (1960) used many experimental data to draw the curves for the cloud amount dependence upon the relative humidity for different atmospheric layers. He showed that f_{cr} is depends upon height, - the larger height, the smaller f_{cr} value.

The great experience existed in Russia from the regular aircraft observed data supports this conclusion. The analyses of the aircraft data were carried out by Gogoleva (1956), Reshetov (1962), Abramovich (1964). They used the dew point deficit, Δ, as the best characteristic of the moist air proximity to the saturation state. They found that Δ values within the cloud are in limits of $1° \div 5°$ in dependence of height. Aircraft information and curves presented by Smagorinsky are the objective results for the real atmospheric situations.

The wide spread cloud parameterization methods used in hydrodynamical atmospheric models are based upon the prescribed f_{cr} values. The another approach to cloud amount parameterization doesn't exist now. This problem isn't correct because it is necessary to describe the cloud amount distribution inside the model grid cell knowing the humidity characteristics in the center of the cell only. To solve this problem some hypothesis are needed.

All cloud amount parameterizations used today have very different vertical distribution of f_{cr} as a model tuning parameter. Comparison of different cloud amount parameterization methods was carried out by Kurbatkin et al. (1988) under the same initial data. The discrepancy of cloud amount in different models was very great in limits of $0.2 \div 0.8$. It is evident that every parameterization is tuning radiation fluxes at top of the model atmosphere. So the cloud parameterization methods are model depended and aren't objective.

Sundqvist (1978) proposed the new hypothesis of humidity characteristics distribution inside of model grid cell in dependence of cloud amount. This idea was applied to dew point deficit as the Humidity transformation model developed in Hydrometeorological center of Russia includes the transfer equation for this characteristic (Dmitrieva-Arrago et al., 1985, 1996,1998). We proposed that in every grid point:

$$\Delta = \Delta_{cr}(1 - C) + C\Delta_{cl}, \tag{1}$$

where C is a cloud amount, Δ_{cr} is Δ critical value for the cloud formation starting and Δ_{cl} is Δ in cloudy part of the cell.

The scheme of this parameterization is presented on Fig.1. We assume that after the cloud formation beginning the value of Δ_{cr} is remained in cloudless part of the cell. The expression for cloud amount follows from (1) for every model level:

$$C = \frac{\Delta_{cr} - \Delta}{\Delta_{cr} - \Delta_{cl}} \tag{2}$$

Formula (2) may be applied to model predicted Δ value or to observation data to check the proposed method of cloud amount parameterization. We have used the set of radiosonde data of relative humidity and temperature vertical distribution for the European region of Russia for September and October 2000 (638 cases). The radiosonde data were accompanied by synoptic observation of the general cloud amount.

The vertical distribution of Δ was calculated using the radiosonde data. Needed Δ_{cr} values for (1) were calculated using the prescribed f_{cr} vertical distribution (Table 1) taken in accordance with analyses of aircraft data and Smagorinsky results. Than the general cloud amount was computed and compared with observed synoptic data using the method developed by Veselova (1988). The results of comparison are presented in Table 2 and 3. Here in Tables: $\tilde{\delta}$ is mean systematic (arithmetic) error, $\bar{\delta}$ is mean absolute error, σ is standard deviation, $P = N_i/N$, N_i is a number of results in the prescribed interval of mean absolute error, N is general number of cases. The mean absolute error intervals were taken as $\bar{\delta} \le 0.1, \le 0.2, \le 0.3, \le 0.4$.

The results of calculation of skill criteria values are in limits of 0.3÷0.4 for this set of data.

The Tables 2 and 3 and received skill criteria values show that the proposed parameterization for the general cloud amount may be evaluated as satisfactory method in limits of error of 0.2.

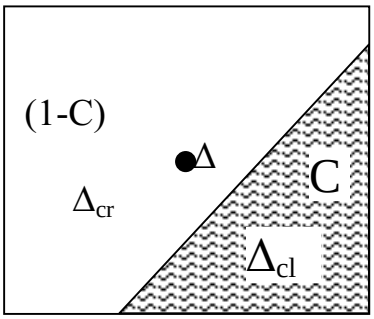

Fig.1

Table1

Vertical distribution of f_{cr}

P,gPa	925	850	700	500	400	300
f_{cr}	0,7	0,7	0,6	0,5	0,4	0,3

Table 2

Mean values of general cloud amount

Month	Number of cases	Observed values	Calculated values
September	318	0.67	0.80
October	320	0.78	0.85

Table 3

Cloud amount calculation errors

Month	$\bar{\delta}$	σ	$\tilde{\delta}$	P, %			
				≤0.1	≤0.2	≤0.3	≤0.4
September	0.22	0.35	0.13	43	68	75	78
October	0.19	0.32	0.07	48	73	80	84

Reference

Abramovich K.G., 1964: Some features of meteorological elements distribution in lower troposphere during cloudy and clear days. Trudy of CIF, 136.

Gogoleva E.I., 1956: Low level cloudiness appearance conditions in European part of USSR and possibility of its forecast. Hydrometeoizdat.

Dmitrieva-Arrago L.R., O.P.Srotzkaya, 1985: Numerical modeling of layer cloudiness. Meteorology and Hydrology, 11.

Dmitrieva-Arrago, L.R., Akimov I.V., 1996: On precipitation formation criteria for non-convective clouds in weather forecast models. Meteorology and Hydrology, 8.

Dmitrieva-Arrago, L.R., Akimov I.V., 1998: Modeling of the cloud water content distribution and influence of its initial data on precipitation forecast. Proceedings of the First WCRP International Conference on Reanalyses, USA, WCRP-104

Kurbatkin G.P., L.R.Dmitrieva-Arrago, S.A.Filatov, 1988: On cloud parameterization in hydrodynamic models of large-scale atmospheric movements. Meteorology and Hydrology, 5.

Reshetov A.A., 1962: High level cloudiness. Meteorology and Hydrology, 4.

Sundqvist H.A., 1978: Parameterization scheme for non-convective condensation including prediction of cloud water content. Q.J.R.M.S., 104

Smagorinsky, J., 1960: On the dynamical prediction of large scale condensation by numerical methods, Monograph, 5, American Geophysical Union, Physics of precipitation.

Veselova G.K., 1988: The method for skill score evaluation for cloud amount forecast. Information bulletin, 26, Hydrometeoizdart

First validation of the prognostic cloud ice scheme in the global model GME

G. Doms, D. Majewski, A. Müller and B. Ritter
Deutscher Wetterdienst, 63067 Offenbach, Germany
e-mail: guenther.doms@dwd.de, detlev.majewski@dwd.de,
aurelia.mueller@dwd.de, bodo.ritter@dwd.de

The operational parameterization scheme of GME for the formation of grid-scale clouds and precipitation is based on a Kessler-type bulk formulation and uses a specific grouping of various cloud and precipitation particles into broad categories of water substance. The particles in these categories interact by various microphysical processes which are parameterized in terms of the mixing ratios as the dependent model variables. Four categories of water substance are considered: water vapour, cloud water, rain and snow. Cloud water is treated as bulk phase with no appreciable terminal fall velocity relative to the airflow, whereas single-parameter exponential size-spectra and empirical size-dependent terminal fall velocities are assumed for raindrops and snow crystals. The calculation of cloud water condensation and evaporation is based on instantaneous adjustment to water saturation. This leads to a number of drawbacks of the scheme, namely

- Clouds will always exist at water saturation independent of temperature.
- The cloud ice-phase is neglected by assuming a fast transformation from cloud water to snow.
- Contrary to observations high level humidity exceeding ice saturation is often predicted by GME.

To overcome these problems, a new scheme including prognostic cloud ice has been developed.

This parameterization scheme was designed to take into account cloud ice by a separate prognostic budget equation. Cloud ice is assumed to be in the form of small hexagonal plates that are suspended in the air and have no appreciable fall velocity. As a novel feature of the scheme, we formulate the depositional growth of cloud ice as a non-equilibrium process and require, at all temperatures, saturation with respect to water for cloud liquid water to exist. Ice crystals which are nucleated in a water saturated environment will then grow very quickly by deposition at the expense of cloud droplets. Depending on local dynamic conditions, the cloud water will either evaporate completely, or saturation will be maintained, resulting in a mixed phase cloud. In case of a comparatively weak forcing, the cloud will rapidly glaciate to become an ice cloud existing at or near ice saturation. Fig. 1 gives an overview on the hydrological cycle and the microphysical processes considered by the scheme.

For a first validation the operational model (Routine) and GME with prognostic cloud ice (Experiment) have been compared with observations (NOAA 15 measurements) for the period September 2000 until August 2001. On the first of each month for this period 30-day GME forecasts starting from analysed initial conditions with fixed SST have been performed. The twelve 30-day runs have been averaged to form an annual mean value. Fig. 2 compares the zonal average of the outgoing longwave radiation (OLR, W/m^2) at the top of the atmosphere of both model versions (Routine and Experiment) with the observations. The inclusion of prognostic cloud ice greatly improves the quality of the simulated OLR due to the different radiative properties of cloud ice compared to supercooled cloud water. The globally averaged annual radiation balance (OLR plus solar radiation balance) at the top of the atmosphere is almost closed in GME with prognostic cloud ice (+2.1 W/m^2) compared with -19.7 W/m^2 for the current operational model. Since January 2, 2002 a parallel test suite of GME with prognostic cloud ice has been established, and an operational introduction is scheduled for April 2002. At the same time prognostic cloud ice will be introduced in DWD's regional model LM as well as in LMs at Meteo Swiss (Switzerland),

SMR-ARPA (Italy), HNMS (Greece) and IMGW (Poland), and in ten HRMs (High resolution Regional Model of the DWD) running world wide e.g. in Brazil, China, Israel, Italy, Oman, Romania, Spain and Vietnam.

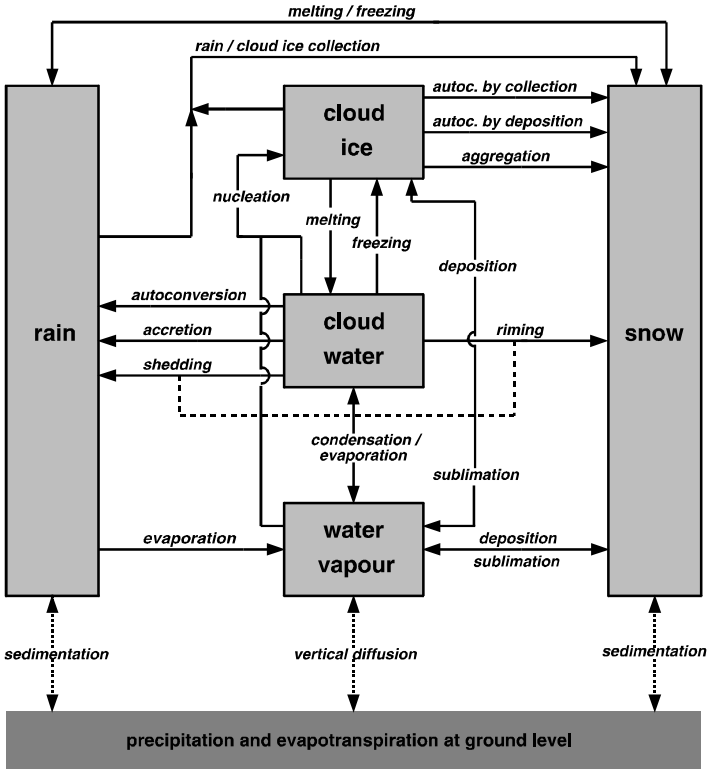

Fig. 1 Hydrological cycle and microphysical processes in the cloud ice scheme

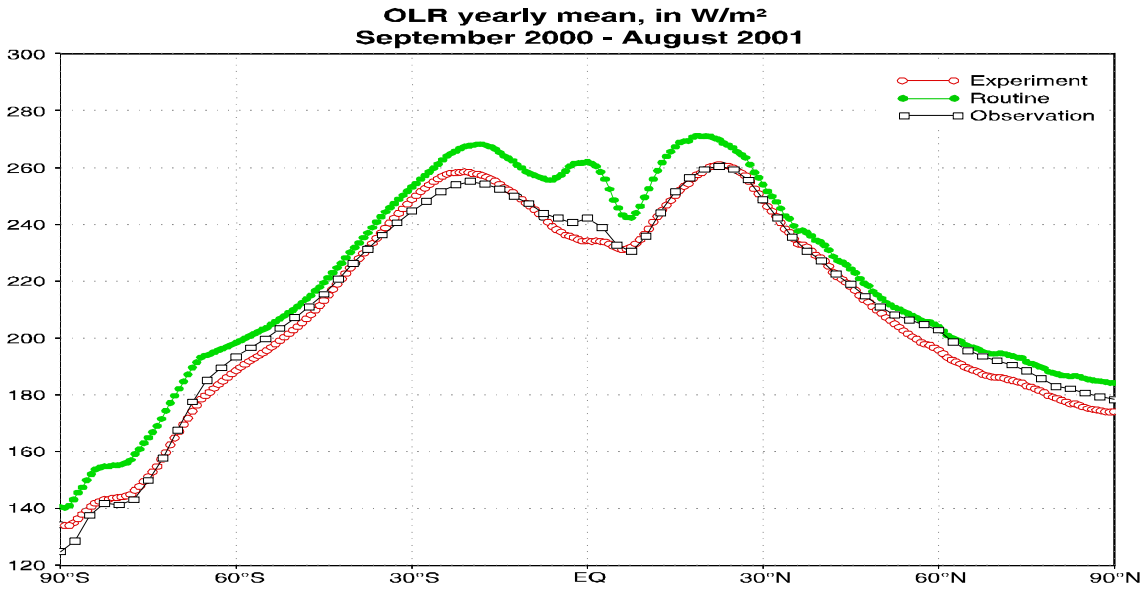

Fig. 2 Zonal mean of outgoing longwave radiation (W/m^2) at the top of the atmosphere

A multi-layer soil model including freezing/melting processes

Erdmann Heise and Reinhold Schrodin

Deutscher Wetterdienst, Research and Development
PO-Box 100465, 63004 Offenbach, Germany
E-mail: Erdmann.Heise@dwd.de, Reinhold.Schrodin@dwd.de

In the present operational models of the German Weather Service the soil heat and water transport processes are calculated by an economic two-layer soil model. The upper layer of this model has a thickness of the order of 0.1 m. In winter large amounts of water/ice available in such a thick layer would result in an exaggerated suppression of temperature changes in the soil - and therefore also in the lowest atmospheric layer - if freezing/melting processes were included. Therefore they were neglected in the present model versions. But, conversely, this leads to daily temperature amplitudes being considerably too large in winter, if freezing/melting processes occur in reality.

To reduce this deficiency, a multi-layer soil model was implemented in the non-hydrostatic limited area model LM of the German Weather Service (Heise and Schrodin, 2002). It allows the choice of thin layers close to the soil surface. In this model the freezing/melting processes are included in two different versions: In the first version complete freezing/melting of soil water/ice occurs at the freezing point temperature. But even with rather thin upper layers the freezing/melting process still seems to be exaggerated. Therefore, in the second version some amount of liquid water may remain in the soil even at temperatures well below the freezing point. The temperature of complete freezing of water is determined dependent on the soil type. This approach basically follows Flerchinger and Saxton (1989).

First experiments simulated a situation of significantly decreasing temperatures in the north-eastern part of Germany (see Figure 1). The prediction of 2m temperatures was verified by observations (obs) at the Meteorological Observatory Lindenberg of the German Weather Service. In the first experiment (mlv) the freezing/melting process in the soil was neglected, leading to temperatures being significantly lower than the observations after 30 h forecast time. In the second experiment (fr0) with total freezing/melting at the freezing point temperature, the diurnal change of temperature is extremely reduced especially in the first 24 hours, showing the too large effect of this version. Only the second version with a variable temperature of complete freezing (frv) yields acceptable diurnal courses of temperature.

References

Heise, E. and R. Schrodin, 2002: Aspects of snow and soil modelling in the operational short range weather prediction models of the German Weather Service. Journal of Computational Technologies. Submitted.

Flerchinger, G. N. and K. E. Saxton, 1989: Simultaneous heat and water model of a freezing snow-residue-soil system. I. Theory and development. Transactions ASAE, Vol. 32(2), 565-571.

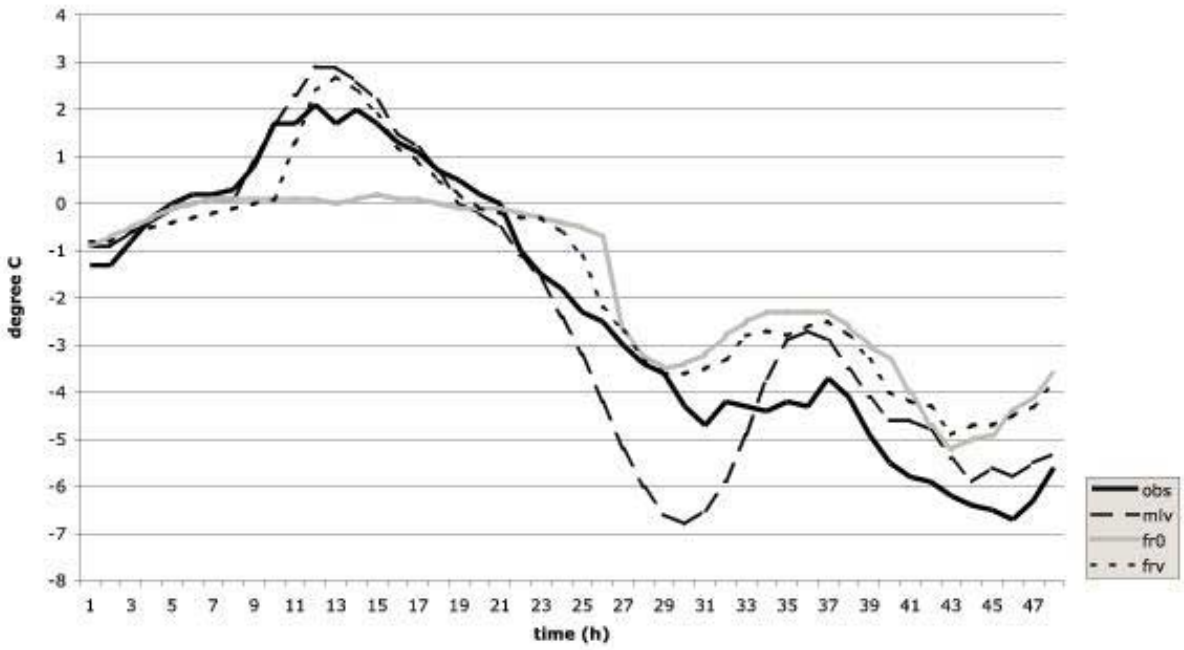

Figure 1: Observed (obs) and predicted 2m temperatures at the Meteorological Observatory Lindenberg of the German Weather Service. 0h corresponds to 28 January 1999 00.00 UTC. See text for details of the three simulations.

Evaluation of a mass-flux convection scheme for mesoscale atmospheric models

Edgar Herrera* and René Laprise

Département des sciences de la Terre et de l'Atmosphère, Université du Québec à Montréal.
*e-mail : herrera@sca.uqam.ca

Introduction

Mesoscale atmospheric models have been used for a wide variety of applications in the environmental sciences during the last two decades. Since greater computing power has become available and the quality of the model simulations has improved as a result of our better understanding of physical processes, the use of Mesoscale atmospheric models has become much more widespread. One of the major physical processes that affects the dynamics and energy of atmospheric circulation systems is the cumulus convection. Hence, it becomes necessary to represent the net effect of an ensemble of convective clouds upon the atmosphere in terms of the grid-scale parameters.

This paper is devoted to the new bulk mass flux convection parameterization for deep and shallow convection developed by Bechtold (Bechtold et al., 2001), hereinafter referred to as Bechtold scheme, employed in a Regional Climate Model (RCM).

Experimental framework

We have chosen the region of Mexico since it includes a tropical climate, a steep topography and, during the fall, heavy precipitations are frequently observed. This constitutes a combination of conditions rarely present in a RCM simulation. The simulation was carried out with the Canadian RCM (Caya and Laprise, 1999) for fall 1989 with a 15 min. timestep. The computational domain is centered over central Mexico, with 130 by 100 grid points in the horizontal with nominal grid spacing of 45 km, and 20 Gal-Chen scaled-height layers in the vertical.

In order to validate the convection scheme, we have compared its performance with that of the Kain-Fritsch (KF) scheme (Kain and Fristsch, 1990) and the dataset of monthly terrestrial surface climate from CRU (New et al., 2000). Both convective schemes, Bechtold and Kain-Fritsch, have a closure assumption based on the removal of the Convective Available Potential Energy (CAPE). Their cumulus cloud model formulation uses a one-dimensional entraining/detraining plume. The stratiform component of the precipitation is obtained from the large-scale condensation part of the second-generation general circulation model (GCMii, McFarlane et al., 1992). The RCM was driven by the NCEP (National Centers for Environmental Prediction) reanalysis at the lateral boundary.

Results

Figure 1 shows the distribution of the fall-mean precipitation, as simulated by the CRCM with the KF and the Bechtold schemes. This pattern shows a correspondence between the simulations and actual observations of the relative maxima, although there is a clear over-estimation over the region of Central America. There is also a strong modulation of precipitation due to the topography. The CRU data of the southern coast of USA show a precipitation maximum of up to 15 mm/day, while KF shows 10 mm/day and Bechtold 6 mm/day. This is a region where the high density of meteorological stations provides a strong support to the CRU dataset. The CRU data of southwestern USA, northern and central Mexico, show a precipitation minimum of 2 to 3 mm/day, which is reproduced by the CRCM with (slightly lower) values of 0 to 1 mm/day. The maximum value over the region of Guatemala is clearly localized and attains values over 4 mm/day with KF and 7 mm/day with Bechtold, which are very close to the actual observations. The average values of the models over the desertic region of Southwestern USA, North and Central Mexico, are 1 to 2 mm/day which differ from the actual observations by only ±1 mm/day. In the region of Cuba, it is only possible to compare the values of the models over a small fraction of the island given the resolution of the ground-cover of the CRU data which has values of up to 5 mm/day, KF presents values of up to 6 mm/day and Bechtold of up to 10 mm/day. By comparing both schemes we see that KF is noisier that Bechtold, which can be clearly observed over Southeastern USA, Northern and Central Mexico. Hence, the convection parameterization of Bechtold gives an efficient and reasonable numerical description of atmospheric convection.

References

Bechtold, P., E. Bazile, F. Guichard, P. Mascart, and E. Richard, 2001: A mass flux convection scheme for regional and global models. *Q. J. R. Meteorol. Soc.*, **127**, 869-886.

Caya, D., and R. Laprise, 1999: A semi-Lagrangian semi-implicit regional climate model: The Canadian RCM. *Mon. Wea. Rev.*, **127**, 341-362.

Kain, J. S., and J. M. Fritsch, 1990: A One-Dimensional Entraining/Detraining Plume Model and its application in convective parameterization. *J. Atmos. Sci.*, **47**, 2784-2802.

McFarlane, N. A., G. J. Boer, J.-P. Blanchet, and M. Lazare, 1992: The Canadian Climate Centre second generation general circulation model and its equilibrium climate. *J. Climate*, **5**, 1013-1044.

New, M. G., M. Hulme, and P. D. Jones, 2000: Representing twentieth-century space-time climate variability. Part II: Development of a 1901-96 monthly grids of terrestrial climate. *J. Climate*, **13**, 2217-2238.

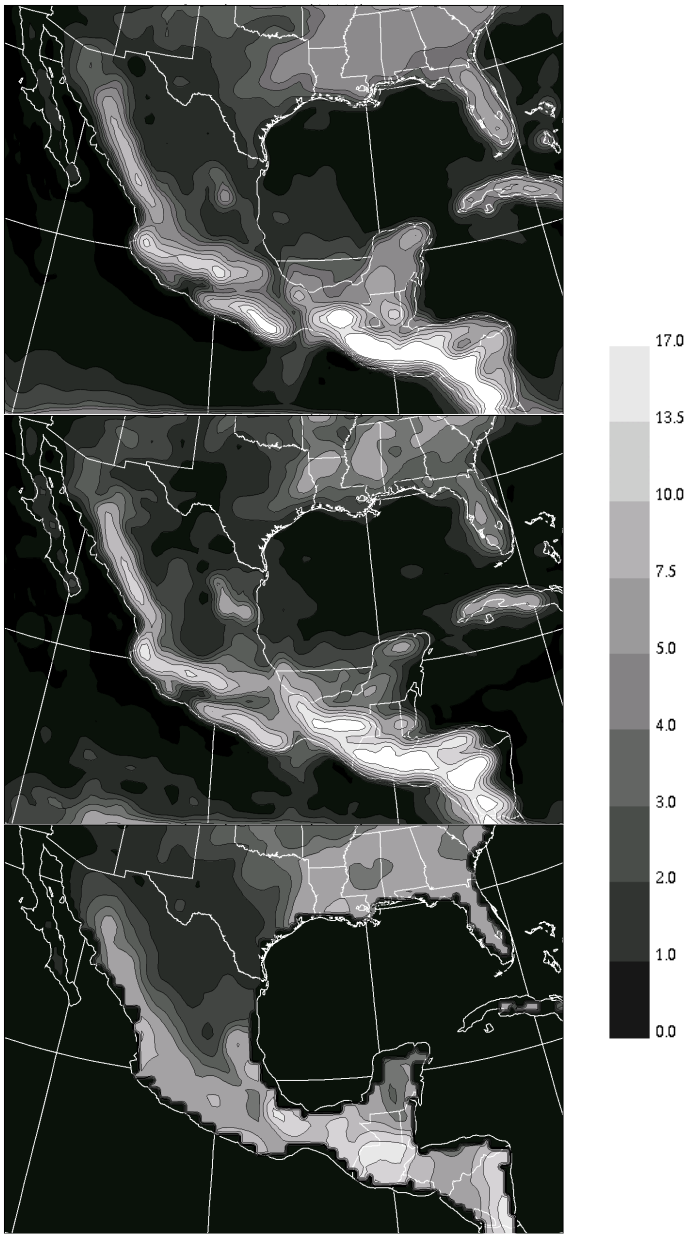

Figure 1. Fall-mean precipitation simulated by the CRCM using the scheme of Bechtold (top), of Kain-Fritsch (middle), and observed climatology from CRU (bottom). Units are in mm/day, contoured at values of 1, 2, 3, 4, 5, 7.5, 10, 13.5 and 17 mm/day.

Impact of a Revised Parameterization of Cloud Radiative Forcings on Earth's Radiation Budgets Simulation

Hiroto Kitagawa* and Syoukichi Yabu

Japan Meteorological Agency, Tokyo, Japan

It is widely recognized that the earth's radiation budget strongly depends on cloud parameters such as fractional coverage, vertical overlapping and radiative properties. Therefore, a good parameterization of the cloud radiative forcings (CRFs) is fundamental to realistically represent the earth's radiations in numerical models. A revised parameterization scheme is proposed for the accurate description of cloud-radiation processes, and its impact on the simulation of earth's radiation budgets is investigated using the JMA operational global NWP model (GSM0103). The revisions include

- The maximum-random cloud overlap assumption proposed by Geleyn and Hollingsworth (1979) is applied to the radiation computations both for longwave (LW) and for shortwave (SW).
- To eliminate the underestimation of LW CRF depending on model's vertical resolution, LW cloud emissivity is evaluated by the sophisticated method suggested by Räisänen (1998).
- SW multiple reflection between layers partially covered by clouds is properly computed by accounting for a vertical overlapping of clouds. This procedure of SW computations is perfectly consistent with the treatment of overlapping clouds in LW computations.
- Following Sun and Rikus (1999), effective radii of ice cloud particles are parameterized as a function of the ice water content and the cloud temperature.

The top of the atmosphere (TOA) radiation fields produced by the model are compared with the Earth Radiation Budget Experiment (ERBE) data. Fig.1 shows the errors in TOA outgoing longwave radiation (OLR) derived from one-month model integrations using the original and revised parameterizations. OLR is very sensitive to the radiative forcing of optically-thin high-level clouds such as cirrus clouds. The sophisticated treatment of cloud emissivity in the revised scheme is able to more precisely evaluate the radiative effect of semi-transparent clouds than the method in the original scheme. Moreover, the new parameterization for effective radii of ice particles increases LW optical depth of ice clouds all over the globe. As a consequence of them, the revised parameterization scheme alleviates the underestimation of LW CRF and somewhat reduces the positive OLR bias.

Fig.2 shows the errors in TOA absorbed solar radiation (net downward SW radiation) simulated by using the original and revised parameterizations. In SW computations, the original scheme assumes the random cloud overlap within a cloudy fraction of model's grid for computational efficiency. However, this approach may lead to too much SW reflection over the convective regions where clouds tend to overlap maximally in the vertical. Over the maritime continent and the ITCZ, the revised scheme substantially suppresses excessive SW cloud forcings and gives a better agreement of TOA SW fluxes with the observation. While the model-produced SW reflectivity in mid- and high-latitudes still remains to be underestimated in spite of the revisions to SW scheme. The deficiency probably results from the insufficient representation of low-level clouds in the model.

References

Geleyn, J.-F., and A. Hollingsworth, 1979: An economical analytical method for the computation of the interaction between scattering and line absorption of radiation. *Beitr. Phys. Atm.*, **52**, 1-16.

Räisänen, P., 1998: Effective longwave cloud fraction and maximum-random overlap of clouds: A problem and a solution. *Mon. Wea. Rev.*, **126**, 3336-3340.

Sun, Z., and L. Rikus, 1999: Parametrization of effective sizes of cirrus-cloud particles and its verification against observations. *Q. J. R. Meteorol. Soc.*, **125**, 3037-3055.

* *Corresponding author address:* Numerical Prediction Division, Japan Meteorological Agency, 1-3-4 Otemachi, Chiyoda-ku, Tokyo 100-8122, Japan. E-mail: kitagawa@naps.kishou.go.jp

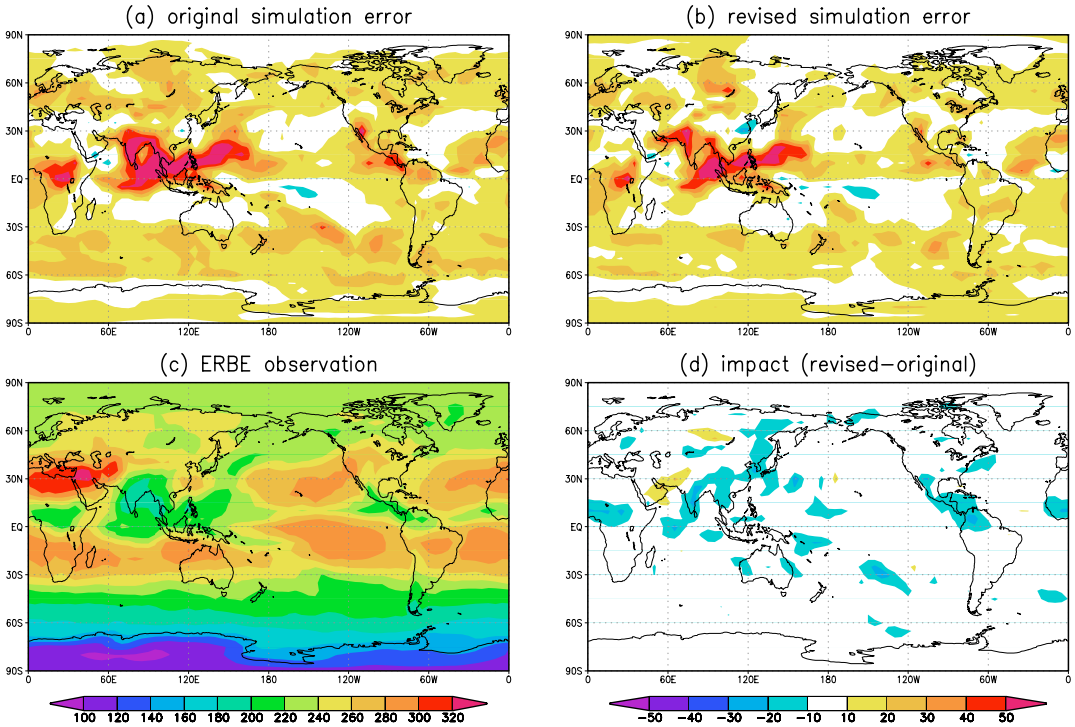

Fig. 1 TOA outgoing longwave radiation (W/m^2) for July 1988. Errors in OLR simulated by using (a) the original scheme and (b) the revised scheme, and (c) the satellite observation (ERBE) and (d) impact of the revisions (revised simulation minus original simulation).

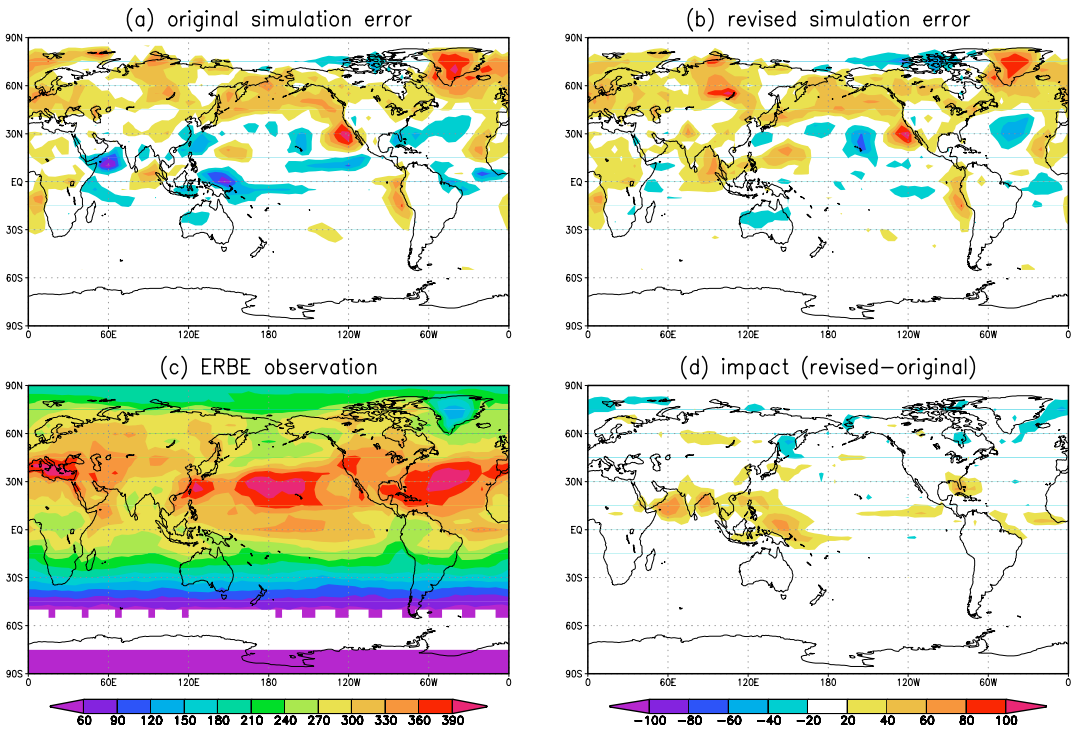

Fig. 2 Same as Fig.1 except for TOA absorbed solar radiation (net downward shortwave radiation).

CORRECTION OF A SURFACE WIND SPEED DUE TO VERTICAL AVERAGING

Gueorgui V. Mostovoi, Pat J. Fitzpatrick and Yongzuo Li
Engineering Research Center, MSU, Stennis Space Center, Mississippi
E-mail: mostovoi@erc.msstate.edu

In regional and global numerical models of atmosphere a vertical momentum flux in a surface layer is expressed as follows *(IFS ECMF, 2001)*:

$$J_u = \rho C_M |U|^2 \quad (1)$$

Where ρ is the surface air density, C_M is the transfer coefficient, which depends on height z_k, (the lowest model level) roughness parameter z_0 and static stability. The wind speed U is determined at z_k. In numerical atmospheric models *(Pielke, 1984)* variables represent an average over grid cell volume. It gives the following expression for the model wind speed U_M at a lowest layer with a thickness of Δz, assuming a unit horizontal cross-section of the cell:

$$U_M = \frac{1}{\Delta z}\int_{Z_0}^{\Delta Z} U(z)dz \quad (2)$$

The layer-averaged U_M value is used in (1) instead of $U(z_k)$ in numerical models. The difference between U_M and $U(z_k)$ values arises from non-linear (logarithmic for the neutral surface layer stratification) variation of a wind speed with a height. There is no difference between U_M and $U(z_k)$ values in a case of the linear variation of a wind speed between model layers. It is easy to show that U_M is always less than $U(z_k)$ value. The ratio between them can be expressed as follows: $U(z_k)/U_M = \ln(z_k/z_0)/[\ln(\Delta z/z_0)-1]$. Use of U_M in (1) will reduce a surface drag force and will cause an overestimation of a surface wind speed.

Expression $[(U(z_k)/U_M)^2 - 1]100$ gives a percentage of increasing in a surface drag force if we will use $U(z_k)$ instead of U_M in (1). This expression is shown in Fig. 1 as a function of z_0 and for z_k = 10m and for Δz = 20m. One can see that this correction to the surface drag force is substantial (20% and more) for relatively high z_0 (more than 0.30m) values.

Sensitivity runs were done using the COAMPS (Hodur, 1997) model to evaluate the significance of this correction. Two-nested domain (27-km and 9-km) and 48 hours "cold-start" run started at December 19 00 UTC were used. The 9-km domain covered Mississippi and Louisiana littoral zone with typical roughness values around 0.3-0.4 m over land. Fig. 2 shows 10-m wind speed forecast at *KPTN* (29.72N, 91.33W) and at *KPQL* (30.46N, 88.53W) produced at 9-km grid for a standard run and for a run with $U(z_k)$ speed used instead of U_M in (1). Use of $U(z_k)$ results in a slight lowering of 10-m wind speed (up to 0.5 m/s) as compare to the standard run.

References

Hodur R.M., 1997: The Naval research laboratory's Coupled Ocean/Atmosphere Mesoscale Prediction System (COAMPS). *Mon. Wea. Rev.*, **125**, 1414-1430.

Pielke R.A., 1984: Mesoscale Meteorological Modeling. AP, 612 pp.

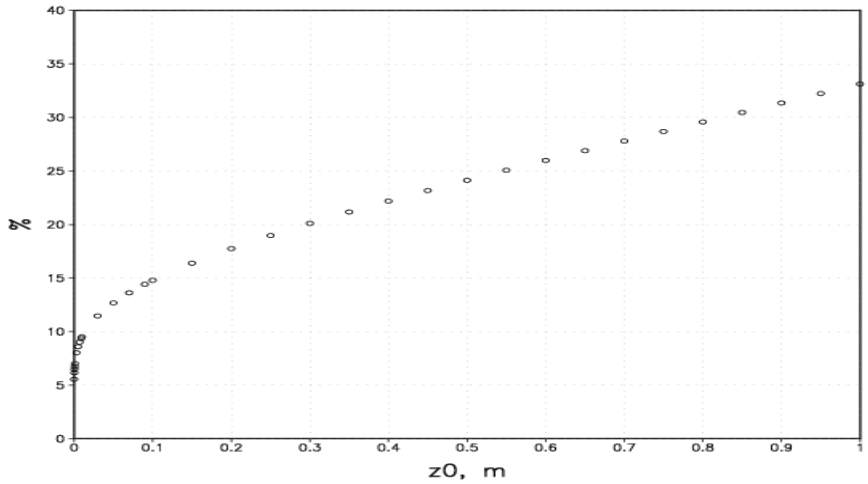

IFS documentation (CY21r4), 2001: Available online at http://www.ecmf.int/research/ifsdocs/index.html.

Fig. 1. $[(U(z_k)/U_M)^2 - 1]100$ as a function of a roughness parameter.

Fig. 2. 10-m wind speed from the standard COAMPS forecast (o) and from the forecast which takes into account effect of a wind speed vertical averaging in estimation of a drag force (•). *KPTN* (a) and *KPQL* (b).

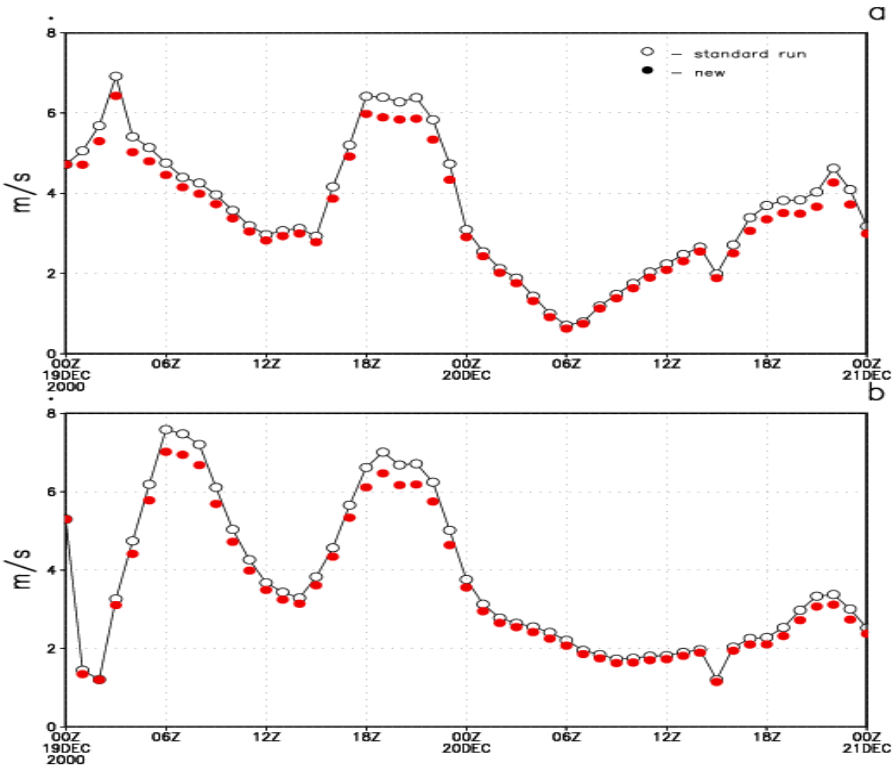

A GLOBAL BIOPHYSICAL MODEL OF ^{18}O IN TERRESTRIAL WATER AND CO_2 FLUXES

DAVID NOONE[1], **CHRISTOPHER STILL**[2] **AND WILLIAM RILEY**[3]

[1] *Geological and Planetary Sciences, California Institute of Technology, Pasadena, California, USA*
[2]*Department of Earth and Planetary Science, University of California, Berkeley, California, USA*
[3]*Lawrence Berkeley National Laboratory, Berkeley, California, USA*
(Email: dcn@caltech.edu)

The abundance of ^{18}O in atmospheric CO_2 can potentially differentiate changes in atmospheric CO_2 associated with changes in the terrestrial biosphere from other direct influences such as those from burning fossil fuel, volcanic inputs and oceanic sources. The amount the ^{18}O in atmospheric CO_2 is largely determined by the effect of gross photosynthetic and soil respiratory fluxes. These fluxes are strongly influenced by the isotopic state of the water. As such, the isotopic state of all water pools in the biosphere must be understood, and quantified, to begin to interpret the terrestrial $CO^{18}O$ signal.

The isotopic concentration of precipitation, the input to the terrestrial hydrology, is governed by climatological influences during evaporation, transport, and condensation in association with moist processes in the atmosphere. Net photosynthetic discrimination against $CO^{18}O$ is due to the differential flux of $CO^{18}O$ molecules across leaf stomata. The differentiation arises because the flux into leaves has the atmospheric signature whereas the flux diffusing back out of leaves is equilibrated with the water of the leaf. A similar exchange occurs in soils where respired CO_2 equilibrates with the soil water strata as it diffuses to the surface. Although the isotopic equilibration associated with these processes does not itself change the isotopic state of the water reservoirs, biospheric processes do modify the water isotopes through, for instance, enrichment during soil evaporation and transpiration. Additional terms in the global $CO^{18}O$ budget come from exchange with the stratosphere, biomass burning, and fossil fuel sources.

The NCAR Land Surface Model (Bonin, 1996) has been adapted to simulate globally the isotopic state of all water pools and CO_2 fluxes as an extension of the site level model described by Riley et al. (2002). Prognostic variables include vertically resolved soil water, leaf water and vapor in the canopy. The adaptation for global simulations lead to the inclusion of additional isotopic reservoirs for snow, water intercepted by the canopy and runoff. With these quantities, and knowledge of the CO_2 exchanges, the ecosystem flux of $CO^{18}O$ can be calculated. Detailed analysis shows this formulation is capable of accurately capturing diurnal variations at the canopy level and responds well to recharge by infrequent precipitation events. Here, the model is forced with daily mean data from the isotopic version of the Melbourne University GCM (Noone and Simmonds, 2002). This GCM is capable of providing the ^{18}O concentration of precipitation and atmospheric water vapor required to drive the isotopic biosphere model. Results shown in Figure 1 are the mean annual cycle from a 10-year simulation, at a spatial resolution of 5.6×5.6 degrees, over four geographic regions (North America, Siberia, Equatorial Amazonia and Australia). The results show the simulated canopy vapor is depleted with respect to the precipitation, and reflects the prescribed atmospheric vapor. At high latitudes the annual cycle in precipitation shows more depletion in the cold winter while the tropics have greater depletion in the wet season. In the Amazon the precipitation signal is reflected in all reservoirs. On the other hand, high latitude regions show that leaf water pools are active only once the growing season has commenced. The leaf water represents a balance between replenishment from the soil reservoir and enrichment during transpiration. In Australia, for instance, semi-aridity leads to little replenishment from the roots and very enriched leaf water results due to evapotraspiration of the lighter isotopes in the summer. Similarly, water on the canopy becomes enriched when the humidity

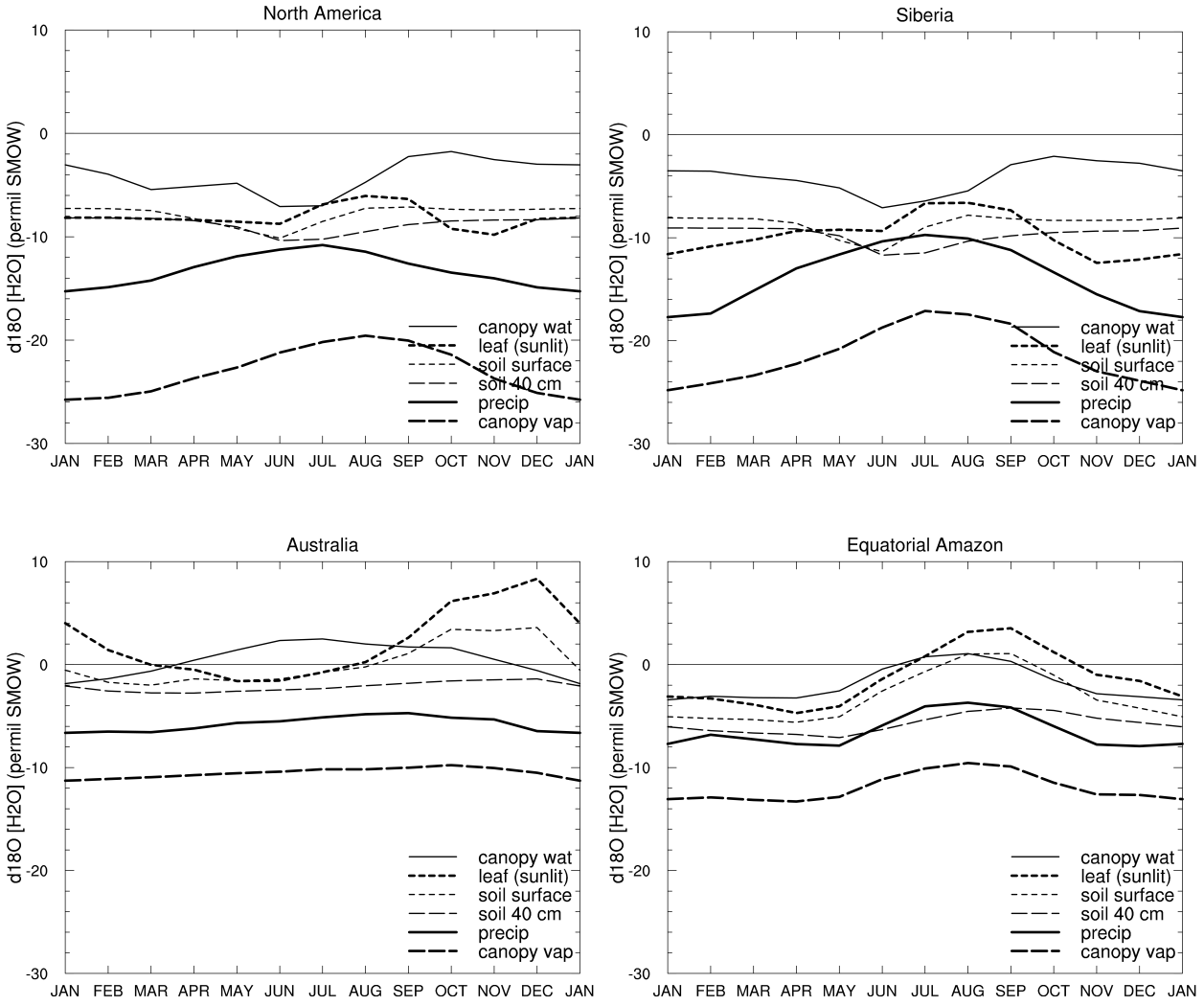

Figure 1: Isotopic concentration of simulated water pools. Data are spatial averages over North America (45-80N), Siberia (45-170E, 45-80N), Equatorial Amazon (30S-10N) and Australia. Isotopic concentrations are shown as "delta" values where $\delta^{18}O=(R/R_{standard})-1$.

is low. Otherwise, it reflects equilibrium with the canopy vapor. The amplitude of the seasonal cycle reduces with depth in the soil water, with deeper layers lagging due to the gravitational drainage.

These initial tests, and detailed tests at individual sites, demonstrate the ability of the model to simulate the main physiological response of the biosphere. Coupling this scheme to an atmospheric GCM is underway to enable direct comparison with the global monitoring networks.

Bonin, G., 1996: A land surface model (LSM version 1.0) for ecological, hydrological and atmospheric studies: Technical description and user's guide, TN-417+STR, NCAR, Boulder, CO.

Noone, D., and I. Simmonds, 2002: Associations between $\delta^{18}O$ of water and climate parameters in a simulation of atmospheric circulation for 1979-1995, *J. Climate*, submitted.

Riley, W. J., C. J. Still, M. S. Torn and J. A. Berry, 2002: A mechanistic model of $H_2{}^{18}O$ and CO_2 fluxes between ecosystems and the atmosphere: model description and sensitivity analyses, *Glob. Biogeochem. Cycles*, submitted.

Diurnal cycle of tropical deep convection: a diagnostic study in ARPEGE

Jean-Marcel Piriou[1], Météo-France/CNRM

Numerical Weather Prediction models or climate models are expected to predict (i) the right mean atmosphere state variables, e.g. temperature fields, (ii) the right mean fluxes, e.g. precipitation fields, and (iii) the right sensitivities and bifurcations, like the response of the atmosphere to a change in the gaseous composition or the right frequency of zonal versus blocking flows over the mid-latitudes. The first question addresses a 0 order problem, with respect to time derivatives: reducing variables biases. The second question addresses a 1st order problem: having the right tendencies for each individual physical process, in the mean time. The third question is the most difficult and is a 2nd order problem: having the right tendencies of the tendencies, i.e. the right bifurcations between meteorological attractors and feedbacks between atmospheric processes.

The way to deal with the first question is to compute biases, useful observations for that purpose are available on the Global Observing System. To deal with the second question, Single Column Modelling and comparisons versus Cloud Resolving Models may be done, and observations now become more offently available from Intensive Observation Periods. Tools to deal with the third question are emerging, and focus on sensitivity aspects and studies of non-stationnary states, like transition from stratocumulus to cumulus regimes, interactions between cyclogenesis and jets in the deepening process, or diurnal cycle.

The Figure compares predicted versus observed diurnal cycle of precipitation in the Tropics: observations[2] show that deep convection peaks in the morning over oceans, and in the evening over continents. The results from both a climate model[2] (University of Reading, Met-Office) and a Numerical Weather Prediction model (Meteo-France) present a quite similar behaviour, and show a large phase lead with respect to observations, on both oceans and continents. This indicates some major problems in individual parameterizations like clear sky turbulence, shallow convection, deep convection, and / or their feedbacks in a continuous transition process.

This kind of diagnostic is a powerful tool to improve our understanding of the atmospheric physics, at least in the tropics. Other related actions are in progress to deal with these 2nd order problems inside NWP and climate models, like the European Cloud Systems project, involving both sensitivity and deep convection diurnal cycle studies, in a SCM versus CRM validation approach.

[1] *Corresponding author address*: J.M. Piriou Météo-France, CNRM/GMAP 42 Av. Coriolis, 31057 Toulouse Cédex, France fax : +33 5 61 07 84 53 email: jean-marcel.piriou@meteo.fr

[2] With the courtesy of Prof. Julia Slingo, The University of Reading, UK

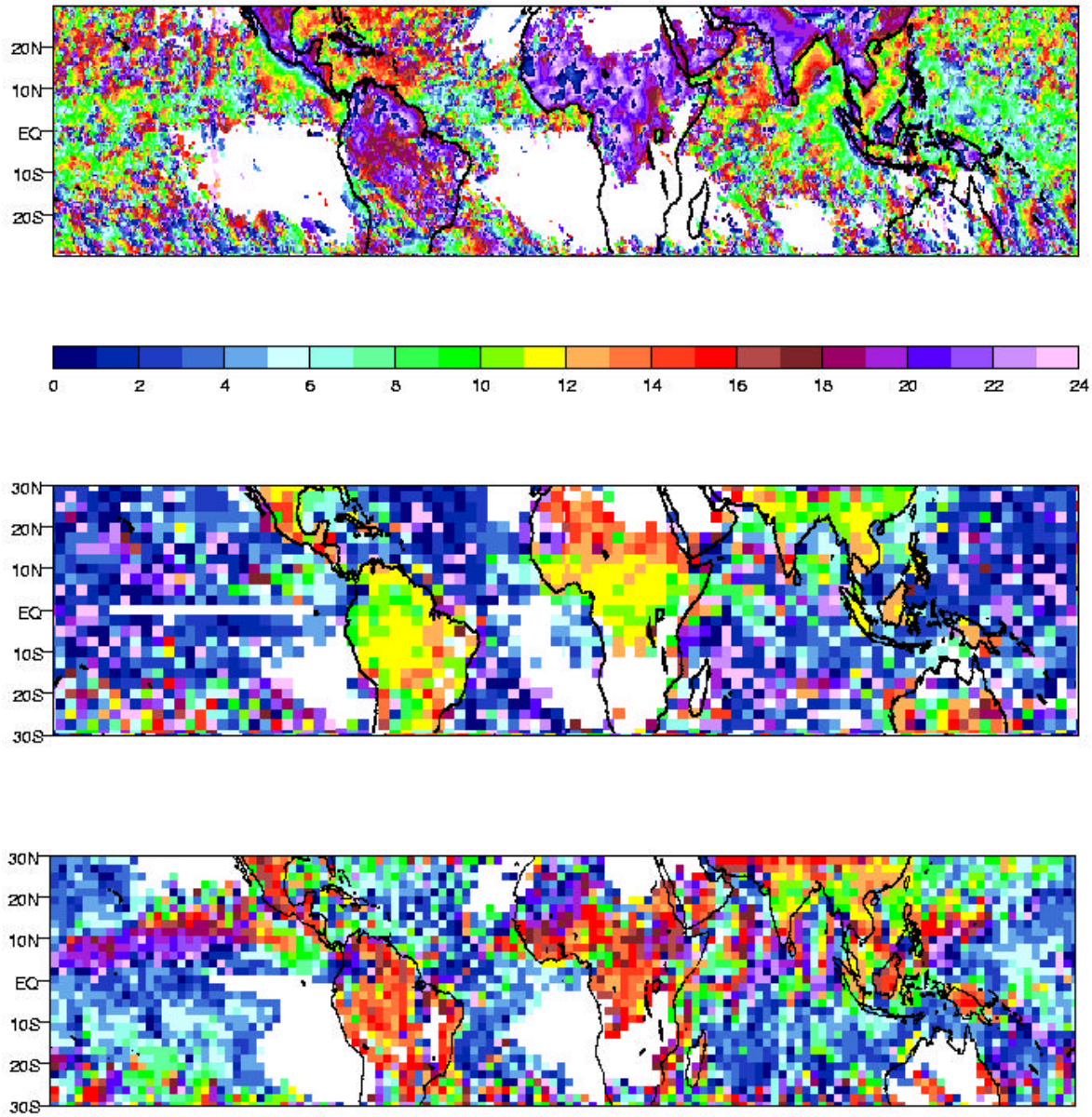

Mean phase of the diurnal harmonic of precipitation for JJA from (a) high resolution satellite window brightness temperatures, (b) the Unified Model (version HadAM3), and (c) the ARPEGE NWP Model. Local solar time of the maximum is given. (a) and (b) with the courtesy of Prof. Julia Slingo, The University of Reading, UK, from the article: Yang and Slingo 2001, Monthly Weather Review Vol. 129, No. 4, pp. 784-801.

Operational implementation of the new turbulence parameterization

Matthias Raschendorfer and Dmitrii Mironov

Deutscher Wetterdienst, Research and Development
PO-Box 100465, 63004 Offenbach, Germany
E-mail: Matthias.Raschendorfer@dwd.de, Dmitrii.Mironov@dwd.de

During the last years a lot of effort was put into the development of a new level 2.5 turbulence parameterization and a new surface layer formulation for the non-hydrostatic limited area model (LM) of the German Weather Service (Raschendorfer, 2001). A great number of test runs as well as a parallel suite to the operational models were used to further examine and tune these new parameterizations. All experiments included the whole data assimilation procedure and the variational soil moisture analysis, which tunes soil moisture content in order to minimise the error of the 2m temperature during clear sky conditions at noon. In order to improve the interpolation of the 2m dewpoint temperature as well, some parameters of the surface scheme were tuned appropriately. The operational verification showed improvements over the then operational versions both in the 2m temperature and in the 2m dewpoint temperature forecasts.

In April 2001 the level 2.5 turbulence parameterization and the new surface scheme became operational. The schemes ran without problems during summer and autumn. In winter some problems occurred with the dewpoint temperature, showing occasionally somewhat too large spread, causing problems in the interpretation of fog. This problem could not yet be finally fixed. In the 2m temperature interpolation in very stable situations sometimes a flip-flop like change between values close to the temperature at the surface or close to the temperature of the lowest prognostic model layer occurred. This could be cured by slightly altering the interpolation procedure.

As an example Figure 1 shows the predicted distribution of turbulent kinetic energy in a cross section covering the lowest 3 km of the model atmosphere. Despite of the only moderate wind speed over land the varying surface height connected with large values of the roughness length produce considerable amounts of turbulent kinetic energy. Conversely, over the Baltic Sea the turbulent kinetic energy remains small although wind speeds are rather high. But even the small height of the northern tip of the isle of Öland in the Baltic Sea (close to horizontal grid point number 270) produces large values of turbulent kinetic energy.

References:

Raschendorfer, Matthias, 2001: The new turbulence parameterization of LM. In: G. Doms and U. Schättler (Edts.): COSMO Newsletter No. 1, 89-97 (available at www.cosmo-model.org).

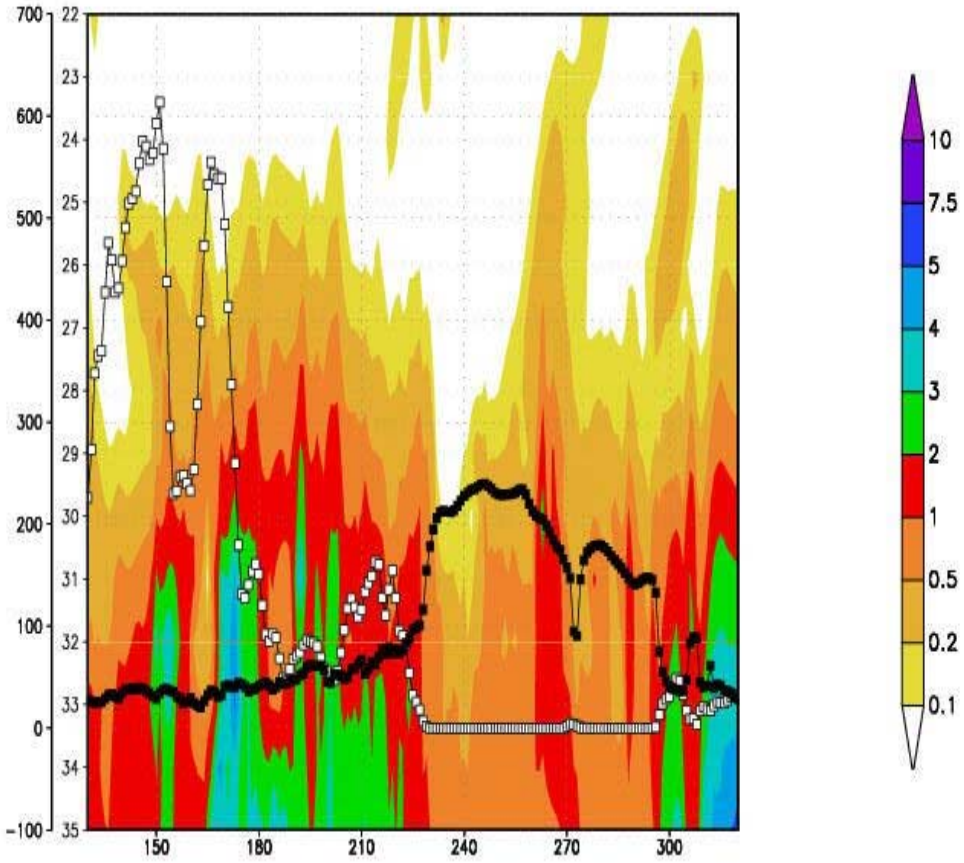

Figure 1: Cross section of predicted turbulent kinetic energy (in J/kg, shaded), predicted wind speed at 10 m height (0.1 m/s, leftmost scale, black squares), and surface height (m, leftmost scale, open squares) along a line from north-western Austria (left) to the Swedish coast of the Baltic Sea (right). The numbers from 22 to 35 represent model layers between 3 km height and the surface, the numbers at the abscissa are model grid points. 12 hours forecast, starting at 21 Dec 2001, 00.00 UTC.

Very short range atmospheric forecasts using a nudging procedure to combine analyses of cloud related variables with a numerical forecast model.

Bent H. Sass (e-mail: bhs@dmi.dk) and
Claus Petersen (e-mail: cp@dmi.dk)

Danish Meteorological Institute
Lyngbyvej 100, DK-2100 Copenhagen , Denmark

February 20, 2002

High forecast accuracy of cloud cover and precipitation is needed in order to make quality predictions of various weather parameters close to the ground. A specific example is the problem of providing accurate local predictions of frost and/or snow on road surfaces. At DMI (Danish Meteorological Institute) a forecast module predicting road conditions (Sass, 1997) has recently been integrated to a version of the atmospheric model DMI-HIRLAM (Sass et al., 2002) used operationally at DMI. In this way an efficient exchange of data between the two models, e.g. cloud and precipitation variables, is possible during model execution. In order to utilize cloud- and precipitation data for assimilation, a nudging procedure is currently being developed which combines a 3-D cloud analysis and a precipitation analysis with a DMI-HIRLAM forecast to improve the quality of short range predictions of cloud cover and precipitation. The production of a 3-D cloud analysis and a precipitation analysis is a non-trivial issue and is currently at an early stage where only conventional data are used in combination with a model first guess. During an assimilation period (1 to 6 hours) prior to a forecast, the cloud and precipitation analyses are assimilated by a tendency modification for both specific humidity and cloud condensate which are both prognostic variables. The tendency modification depends on differences between analysed and forecasted cloud cover and on the difference between analysed and forecasted precipitation. Non-local vertical structures are imposed to incorporate precipitation effects. 1-dimensional tests indicate a considerable skill to adjust model cloud cover and precipitation towards analysed amounts. The assimilated information is retained into the forecast phase. Cloud cover modifications during 1-D asimilation tests extend in many cases with a weak dynamical forcing into a forecast range of more than +12 hours and sometimes beyond +18 hours.

An example of a 3-D assimilated and forecasted total cloud cover for Denmark and surrounding areas is shown in figure 1. The case applies to a situation on 13 December 2001 dominated by low level clouds. The left panel shows the forecast results after nudging was run, and the right panel shows the corresponding results without nudging. When comparing with cloud observations the results using nudging appears to be the most realistic.

Experience indicates that nudging of cloud cover plus precipitation information shows a considerable sensitivity to the methodology applied for the nudging. Furthermore the assimilation appears to be sensitive to the the model physics used in connection with cloud- and precipitation processes.

References

Sass, B. (1997). A numerical forecasting system for the prediction of slippery roads. *J. Appl. Meteor.*, 36:801–817.

Sass, B. H., Nielsen, N. W., Jørgensen, J. U., Amstrup, B., and Kmit, M. (2002). The operational DMI-HIRLAM system. Dmi tech. rep. no. 02-5, Danish Meteorological Institute.

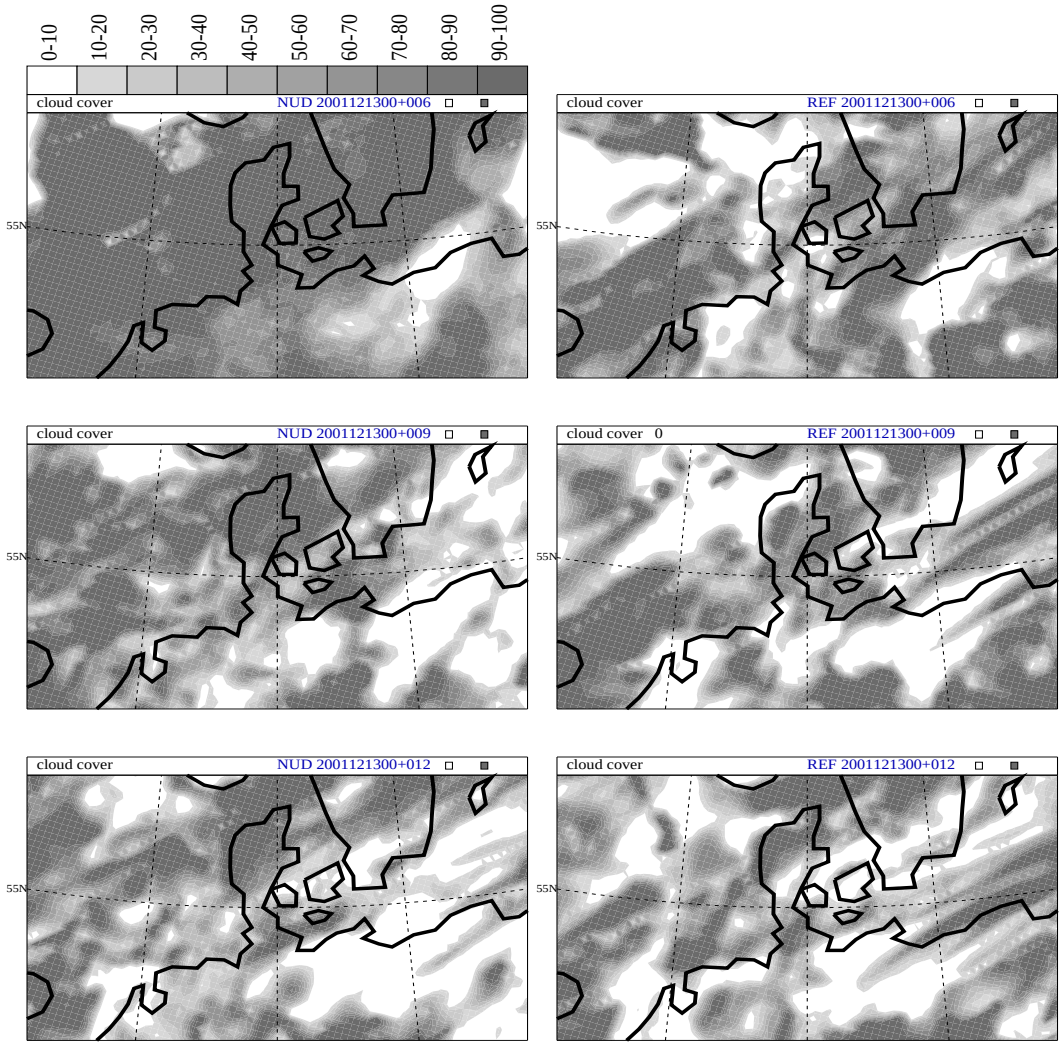

Figure 1: Total cloud cover for 3-D case on 13 December 2001 with nudging applied (NUD) and without nudging (REF). The +006 applies to the end of the nudging period while +009 and +012 correspond to 3 and 6 hours real forecasts.

Two-equation turbulence closure for quantitative description of boundary layers

Shnaydman V.A.
Department of Environmental Sciences, Rutgers University, Cook college, 14 College Farm Rd, New Brunswick, NJ, 08901 USA, e-mail: volf@envsci.rutgers.edu

The introduction of the prediction equations for more and more turbulence quantities is that more physics is taken into account and the various complex turbulence phenomena can the be described [1,3,7]. Now the two-equation turbulence closure which includes the equations of kinetic turbulent energy(TKE) , dissipation rate(epsilon), Kolmogorov-Prandtl and Smagorinsky relationships for vertical and horizontal turbulent exchange has by far achieved the popularity for practical aims as an alternative to use Yamada-Mellor method[2,4,5,6]. Let's emphasize that the aim of described turbulence closure is the reconstruction of 3D distributions of atmospheric transfer and the characteristics of the turbulence in ABL for the service of the ecological monitoring [1]. Now the quantitative description of the air and water pollution problem uses the turbulent diffusion equation in the framework of vertical and horizontal coefficients of turbulence. In considered performance the turbulent closure method has to give a possibility of the definition of the coefficients of the vertical and horizontal turbulent exchange. The expediency of using the equation for TKE is now recognized, but the using equation for epsilon has been criticized because the process of the dissipation is associated with the small-scale turbulence. However, the energy amount dissipated is controlled by the energy fed from the large- scale motion. In this case, the spectral cascade of energy as a flow from the region of energy- carrying eddies determines the absorption of energy in a “dissipative tail”. At the same time, in cascade transfer mechanism the viscosity adjusts itself to the spectral flow by regulating the scale of turbulent eddies. Strictly, the dissipation used in the closure scheme is the rate of energy passed on by the large scales for absorption at smallest scales. Therefore the value of dissipation may be considered as a parameter characterizing the large-scale motion. Using equations for TKE and epsilon it can be possible to describe, at first, the extension of eddies which provides a cascade transfer of energy over the spectrum of scales, the sequential subdivision of eddies and a reduction of their sizes, second, the dissipation destroying the smallest eddies and thereby effectively increasing their characteristic scale.

Thus, the connection of equations for turbulent kinetic energy and for dissipation rate, Kolmogorov-Prandtl relationship are physically well-founded and acceptable closure method for vertical turbulent exchange.

Unlike the coefficient of vertical turbulent exchange, the coefficient of horizontal turbulent exchange is a parameter connected with the scale of division between mean and fluctuation motions, and in this sense it depends on a spatial resolution of the numerical scheme. The definition of horizontal coefficient is based on (1) the division of the motions into large-scale and subgrid scale, (2) the calculation of the kinetic energy production using the horizontal coefficient of turbulence and modulus of deformation, (3) the determination of kinetic energy transfer from large-scale to subgrid-scale motions. These considerations are the basis of Smagorinsky relationship for the horizontal coefficient of the turbulent exchange.

The merit of the closure method is that physically justified boundary conditions are formulated for TKE and epsilon. Equilibrium of the production and dissipation of the turbulent kinetic energy in the roughness sublayer allows to obtain the vertical boundary condition for the turbulent parameters at the roughness level. The turbulent fluxes of TKE and epsilon are given as a small values at the upper level of the calculation domain. The turbulent parameters are calculated with the sufficient accuracy at the lateral boundaries by neglecting the advective terms in the equations of turbulent kinetic energy and of dissipation rate.

At the initial time 3D distribution of the turbulent parameters is reconstructed by hydrodynamical interpolation procedure which represents the solution of 1D stationary equations for turbulent kinetic energy and dissipation rate .

The semi-implicit numerical integration method used the finite difference equations obtained by the forward -differencing scheme for integration in time, the central differences for the terms of advection and centered-in-space differences for the turbulence diffusion terms. The implicit treatment concerns the vertical turbulent exchange terms in the equations and adjusts the small vertical spacing required to resolve the internal structure of boundary layer without drastically reducing the time step as would be with more usual explicit scheme. The use of centered-in-vertical implicit scheme results in a tri-diagonal matrix which is solved by the factorization methods. The linear and finite-difference forms of TKE and epsilon equations are constructed in such way that the solution for TKE and epsilon have to be positive. It concerns the buoyancy and dissipation terms in the turbulence closure equations. If the finite-difference approximation is applied to linear forms of the TKE and epsilon equations constructed the criteria of stability and positive numerical solution are fulfilled.

The above considerations show that the potentialities of described turbulence closure is far from exhausted and can be successfully used to solve the tests of air and water pollution and other applied problems.

References:

1.Bacon, D.P., et. al.: 2000, ‘A Dynamically Adapting Weather and Dispersion Model: The Operational Multiscale Environmental Model with Grid Adaptivity (OMEGA)’. Mon. Wea. Rev.128, 2044-2076.

2.Duynkerke,P.G., Nieuwstadt,F.T.M.:1989, 'A Solution of the E-Epsilon Model for Nearly Homogeneous Turbulence with a Mean Shear', Appl. Sci. Res. 46, 25-43.

3.Canuto,V.M., Dubovikov, M.S.:1996, 'A Dynamical Model for Turbulence. I General Formalism'. Physics of Fluids, 8,587-598.

4.Mellor, G.L. Yamada T.: 1982,'Development of Turbulent Closure Model for Geophysical Fluid Problems’, Rev. Geophys. Space Phys. 20, 851-875.

5.Nakanishi,M.:2001,'Improvement of the Mellor-Yamada Turbulence Closure Model Based on the Large-Eddy Simulation Data' , Boundary-Layer Meteorol. 90, 375-396.

6.Shnaydman, V.A., Tarnopolsky, A.G.:1993, ‘Modeling of a Geophysical Boundary Layer’, Dokl. NAS of Ukraine 9, 114-121.

7.Ying,R.,Canuto,V.M.:1997,'Numerical Simulation of Flow over Two-Dimensional Hills Using a Second-Order Turbulence Closure Model', Boundary-Layer Meteorol. 85, 447-474.

Impact of physical processes in a GCM on the frequency of tropical cyclones

Mitsuru Ueno and Jun Yoshimura
Typhoon Research Department, Meteorological Research Institute
e-mail: mueno@mri-jma.go.jp

A long-term trend of tropical cyclone (TC) frequency under the global warming condition has been a matter of great concern. Some modeling studies predict smaller number of TC genesis under the condition than in the current climate although some contrary results are reported. It is well known that even state-of-the-art GCMs have large uncertainties especially in physical processes such as deep convection, which have large impact on the model behaviour in the tropics.

Aside from the impact of global warming on TC frequency, here in this study we investigate the effect of the two physical processes, cumulus parameterization (CP) and radiative process (RP), on the frequency of modeled TC formation. In the study, a T106-L21 version of the previously operational JMA global model (JMA/NPD 1993, 1997) is used as GCM. The model is integrated for one year with three different combinations of CP and RP (Table 1). RAD-B96 and -S96 differ in several points such as the manner of cloud-overlapping in the vertical, absorbers considered and so on.

Table 1: List of experiments

Experiment ID	Cumulus Parameterization	Radiative process
Exp.A	Kuo-type scheme	RAD-B96 (operational before 1996)
Exp.B	prognostic Arakawa-Shubert scheme	RAD-B96 (operational before 1996)
Exp.C	prognostic Arakawa-Shubert scheme	RAD-S96 (operational since 1996)

Table 2 compares TC frequency among the three experiments for some selected basins. The criteria used to qualify a disturbance as TC in the model is just the same as in Yoshimura et al. (1999). The table clearly demonstrates large sensitivity of TC frequency to both of CP and RP.

Table 2: Frequencies of tropical cyclones simulated by the model

Experiment ID	Northwest Pacific	Northeast Pacific	South Pacific	Global
Exp.A	51	21	18	182
Exp.B	22	2	11	71
Exp.C	5	1	2	25

To gain some insight into how the different schemes might produce different number of TCs, we examine the relationship between the rainfall amount and relative vorticity at low levels, because the former is a direct outcome of convective activities (therefore strongly depends on the formulation of deep convection) and the latter could be a good indicator of vortex spin-up. Model data used for the study has a horizontal resolution of 1.125 degree in longitude and latitude with an interval of 12 hours over the entire integration period. Table 3 shows 12-hour relative vorticity change at 850 hPa ($\varsigma_{t+12} - \varsigma_t$), stratified by the corresponding 12-hour rainfall amount and magnitude of relative voriticity (ς_t), and averaged over any relevant grid points within the basin. Contribution from horizontal advection is subtracted from $\varsigma_{t+12} - \varsigma_t$ to focus

on the vorticity change associated with vertical motion fields. Although we show here the result only for the Northwest Pacific, remarkably larger values in Exp.A are commonly observed in all other basins.

Table 3: 12-hour relative vorticity change at 850 hPa ($10^{-6}s^{-1}$), stratified into several sub-groups according to rainfall amount between t and t+12 hour for $\varsigma_t < 10 \times 10^{-6}s^{-1}$ group.

Experiment ID	12-hour rainfall amount (mm)								
	0 - 5	5 - 10	10 - 15	15 - 20	20 - 25	25 - 30	30 - 35	35 - 40	40 -
Exp.A	+1.7	+7.2	+13.9	+23.5	+35.1	+45.1	+55.9	+67.8	+104.2
Exp.B	+1.0	+4.8	+7.6	+10.3	+11.9	+19.1	+19.0	+22.1	+40.0
Exp.C	+0.4	+2.5	+4.8	+8.9	+13.1	+15.0	+21.6	+30.0	+29.5

Figure 1 shows the latitudinal distribution of annual precipitation for the Northwest Pacific. There is no significant difference between Exps.A and B except for near the equator where TCs rarely form because of minimal Coriolis force there. On the other hand, Exp.C produces much smaller rainfall amounts over theTC genesis area. From the results presented here we can tentatively draw the conclusion that the difference in TC frequency between Exps.A and B might be attributable to the difference in the strength of linkage between vorticity production and convective heating between the two cumulus parameterization schemes. On the other hand, the difference between Exps.B and C might be explained by the difference in large-scale circulation such as Hadley cell yielded by using the different radiation code.

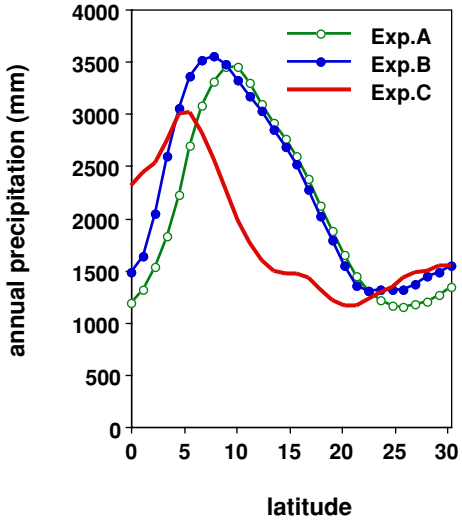

Figure 1: Annual precipitation (mm) simulated by the model over the Northwest Pacific basin.

References

JMA/NPD 1993, 1997: Outline of operational numerical weather prediction at Japan Meteorological Agency. Appendix to progress report on numerical weather prediction.

Yoshimura J., M. Sugi and A. Noda, 1999: Influence of greenhouse warming on tropical cyclone frequency simulated by a high-resolution AGCM. a. Preprints, 23rd Conf. Hurr. Trop. Meteor., Dallas, TX, Amer. Meteor. Soc., Boston, MA 02108, 1081-1082.